Jdp2 downregulates Trp53 transcription to promote leukaemogenesis in the context of Trp53 heterozygosity

Open

Oncogene (2013) 32, 397–402

www.nature.com/onc

SHORT COMMUNICATION

Jdp2 downregulates *Trp53* transcription to promote leukaemogenesis in the context of *Trp53* heterozygosity

L van der Weyden[1], AG Rust[1,4], RE McIntyre[1,4], CD Robles-Espinoza[1], M del Castillo Velasco-Herrera[1], R Strogantsev[2], AC Ferguson-Smith[2], S McCarthy[1], TM Keane[1], MJ Arends[3] and DJ Adams[1]

We performed a genetic screen in mice to identify candidate genes that are associated with leukaemogenesis in the context of *Trp53* heterozygosity. To do this we generated *Trp53* heterozygous mice carrying the *T2/Onc* transposon and *SB11* transposase alleles to allow transposon-mediated insertional mutagenesis to occur. From the resulting leukaemias/lymphomas that developed in these mice, we identified nine loci that are potentially associated with tumour formation in the context of *Trp53* heterozygosity, including *AB041803* and the Jun dimerization protein 2 (*Jdp2).* We show that *Jdp2* transcriptionally regulates the *Trp53* promoter, via an atypical AP-1 site, and that *Jdp2* expression negatively regulates *Trp53* expression levels. This study is the first to identify a genetic mechanism for tumour formation in the context of *Trp53* heterozygosity.

Oncogene (2013) **32,** 397–402; doi:10.1038/onc.2012.56; published online 27 February 2012

Keywords: p53; Jdp2; transposon; heterozygosity; lymphoma; mice

INTRODUCTION

Genetic alterations of *TP53* are frequent events in tumourigenesis and promote genomic instability, impair apoptosis, and contribute to aberrant self-renewal.[1–4] The spectrum of mutations that occur in *TP53* in human cancers is diverse. Missense mutations that deregulate the DNA-binding domain are common, and prevent or impair the transcriptional regulatory activity of *TP53*.[3] Cytogenetic alterations that delete or disrupt *TP53* have also been reported, as has epigenetic silencing due to methylation of the *TP53* promoter.[3] In both carcinomas and haematopoietic malignancies, *TP53* mutation status has been shown to correlate with prognosis.[5,6] *TP53* is generally considered a tumour-suppressor gene,[2] with inactivation of both copies of the gene seen in many tumours. Paradoxically, several studies have observed accelerated tumourigenesis in $Trp53^{+/-}$ mice that develop tumours despite retaining a wild-type copy of *Trp53*.[7–10] Furthermore the analysis of tumours from Li-Fraumeni patients with germline alterations of *TP53,* suggest that a significant proportion may retain a wild-type *TP53* allele.[11–13] Threshold levels of P53 are required for processes such as suppression of apoptosis or induction of cell-cycle arrest.[14] In the context of *TP53* heterozygosity it is possible that transcriptional silencing of the wild-type *TP53* allele by mechanisms such as promoter methylation, altered *cis*-regulation of the gene that decreases transcription from the wild-type *TP53* allele, or post-translational modification of P53, decreases *TP53* function to a level such that tumourigenesis can occur. In this paper we set out to identify, which somatically mutated genes can contribute to tumour formation in the context of *Trp53* heterozygosity. To do this we used mice heterozygous for *Trp53* (as well as *Trp53* wild type and null controls) to genetically dissect this phenomenon focusing on leukaemogenesis as a model system. This analysis allowed us to identify nine loci that are potentially associated with tumour formation in the context of *Trp53* heterozygosity. We show that the Jun dimerization protein 2 (*Jdp2)* is a site frequently targeted by transposon insertion events leading to upregulated *Jdp2* expression and a decrease in *Trp53* expression levels. Further we illustrate that *Jdp2* regulates the *Trp53* promoter via an atypical AP-1 binding site. This study is the first to identify a genetic mechanism for tumour formation in the context of *Trp53* heterozygosity.

RESULTS AND DISCUSSION

Mouse lines carrying the mutant *Trp53* allele, $Trp53^{Tyr}$, which are null for *Trp53*,[15] the *SB* (*Sleeping Beauty*) transposon array, *T2/Onc,*[16] and the *SB* transposase allele, $Rosa26^{SB11}$ (see Dupuy *et al.*[17]) were intercrossed to generate mice that were homozygous, heterozygous or wild type for the $Trp53^{Tyr}$ allele (hereafter referred to as $Trp53^{-/-}$, $Trp53^{+/-}$ or $Trp53^{+/+}$ mice, respectively) with or without *SB* transposition occurring (that is, on a $T2/Onc^{+/Tg}$ $Rosa26^{+/SB11}$ or $T2/Onc^{+/+}$, $Rosa26^{+/SB11}$ background, respectively). These mice were aged until they became moribund, and, as expected, *SB* transposition significantly accelerated tumour latency in mice of all genotypes (Figure 1a). The predominant tumour type of all genotypes was a widely disseminated $CD3^+$ T-cell lymphoma (Figures 1b and c). A number of solid tumours, mainly undifferentiated sarcomas, were also observed, but only in $Trp53^{+/-}$ or $Trp53^{-/-}$ mice (Figures 1b and c).

Genomic DNA from 36 $Trp53^{+/+}$, 116 $Trp53^{+/-}$ and 9 $Trp53^{-/-}$ SB-induced leukaemic/lymphomic tissues (typically spleen, thymus or lymph node) was extracted and subjected to a previously described linker-mediated PCR approach[18] to amplify barcoded genomic fragments containing transposon–genome junction sequences. These products were then pooled and sequenced on the 454 platform, from which we generated 487 586 uniquely mapped sequence reads (approximately 3000 per tumour). After merging overlapping reads originating from the same sample and removing any on chromosome 1 (because SB

[1]The Wellcome Trust Sanger Institute, Cambridge, UK; [2]Department of Physiology, Development & Neuroscience, University of Cambridge, Cambridge, UK and [3]Department of Pathology, University of Cambridge, Addenbrooke's Hospital, Cambridge, UK. [4]These authors contributed equally to this work. Correspondence: Dr DJ Adams, Experimental Cancer Genetics, The Wellcome Trust Sanger Institute, Wellcome Trust Genome Campus, Hinxton, Cambs, CB10 1HH, UK. E-mail: da1@sanger.ac.uk
Received 28 August 2011; revised 22 December 2011; accepted 13 January 2012; published online 27 February 2012

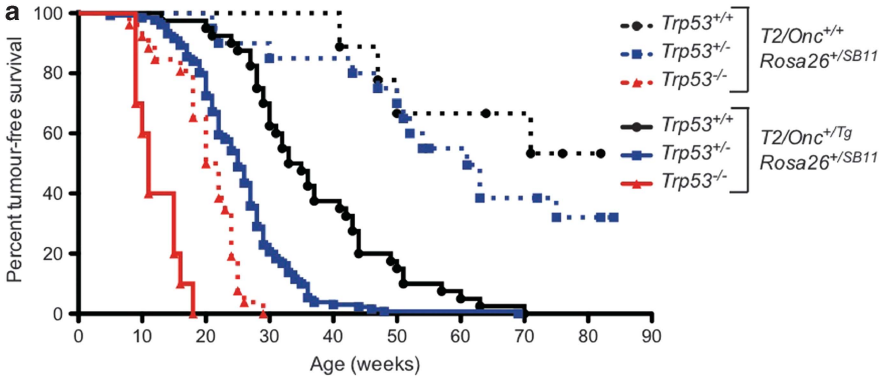

b

Tumor type	*Trp53*$^{+/+}$	*Trp53*$^{+/-}$	*Trp53*$^{-/-}$
Lymphoma (total)	36 (90%)	116 (89%)	9 (90%)
B-cell (CD45R^{+})	0	3	0
T-cell (CD3^{+})	32	80	7
Double positive	4	11	1
Double negative	0	17	1
Solid tumours (total)	0 (0%)	9 (7%)	5 (50%)
Undifferentiated sarcoma	0	5	5
Osteogenic sarcoma	0	2	0
Pancreatic carcinoma	0	1	0
Harderian gland adenocarcinoma	0	1	0

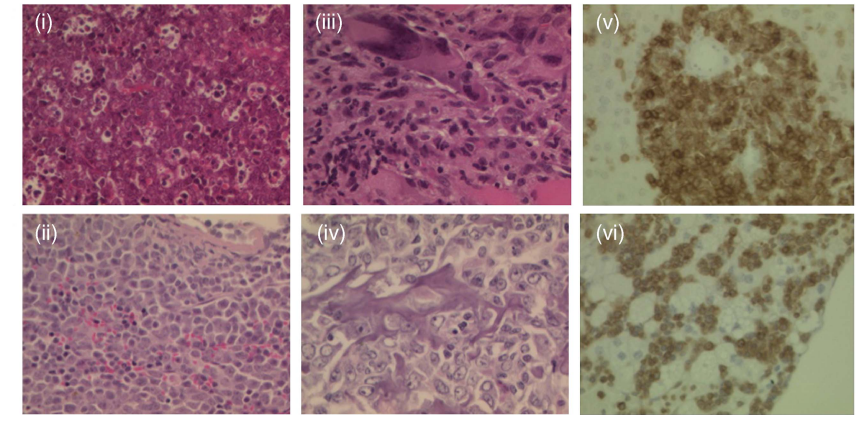

Figure 1. Loss of *Trp53* promotes tumourigenesis. (**a**) Kaplan–Meier curves showing the tumour latency in *Trp53*$^{+/+}$, *Trp53*$^{+/-}$ and *Trp53*$^{-/-}$ mice on a transposon 'jumping' background (that is, *T2/Onc*$^{+/Tg}$ *Rosa*$^{+/SB11}$ solid lines) and 'non-jumping' control background (that is, *T2Onc*$^{+/+}$; *Rosa26*$^{+/SB11}$ dashed lines). Curve comparison using the log-rank (Mantel–Cox) test: $P<0.0001$ for *Trp53*$^{+/+}$ vs *Trp53*$^{+/-}$ vs *Trp53*$^{-/-}$ mice on a 'jumping' background. (**b**) Categorisation of the malignancies developed by the *Trp53*$^{+/+}$, *Trp53*$^{+/-}$ and *Trp53*$^{-/-}$ mice on a 'jumping' background according to the tumour type. Several mice had multiple tumour types. Numbers in brackets represent the percentage of mice developing a specific tumour type as a proportion of the genotype. (**c**) Representative photomicrographs of formalin-fixed, hematoxylin- and eosin-stained sections of (i) thymic lymphoma, (ii) splenic lymphoma, (iii) undifferentiated sarcoma and (iv) osteosarcoma. Representative photomicrographs of immunohistochemically-stained liver sections infiltrated by lymphomas of (v) B-cell origin (CD45R^{+}) or (vi) T-cell origin (CD3^{+}). Immunohistochemistry was performed on formalin-fixed, paraffin-embedded tissue sections that had undergone antigen retrieval (microwaving in high pH citrate buffer for 3×5 min) using rabbit anti-human polyclonal CD3 antibody (Dako, Ely, UK) and rat anti-mouse/human monoclonal B220/CD45R antibody (BD Biosciences, Oxford, UK). The immunohistochemical signal was detected using a secondary biotinylated goat anti-rabbit or anti-rat antibody (Vector Laboratories, Burlingame, CA, USA), using the Vectorstain Elite ABC kit (Vector Laboratories) according to the manufacturer's instructions. All sections shown are representative and images are at $\times 400$ magnification.

transposons frequently reintegrate into regions adjacent to the donor locus–a phenomenon known as 'local hopping'[16]), we obtained 7538 (*Trp53*$^{+/+}$), 21 975 (*Trp53*$^{+/-}$) and 1829 (*Trp53*$^{-/-}$) unique, non-redundant insertion sites (for the respective tumour genotypes indicated in brackets). Using a previously described Gaussian Kernel Convolution statistical method for determining common insertion sites (CISs),[19,20] we identified 42, 63 and 9 CISs in *Trp53*$^{+/+}$, *Trp53*$^{+/-}$ and *Trp53*$^{-/-}$ tumours, respectively, ($P<0.05$ on a chromosome-adjusted scale; Figure 2 and Supplementary Table 1). Many of these genes have been previously implicated in the pathogenesis of T-cell lymphomagenesis/leukaemogenesis, including *NOTCH1*, *PTEN* and *IKZF1* (reviewed in Demarest *et al.*[21]). There were 12 CIS genes in common between the *Trp53*$^{+/+}$ and *Trp53*$^{+/-}$ tumours, specifically *Mecom*

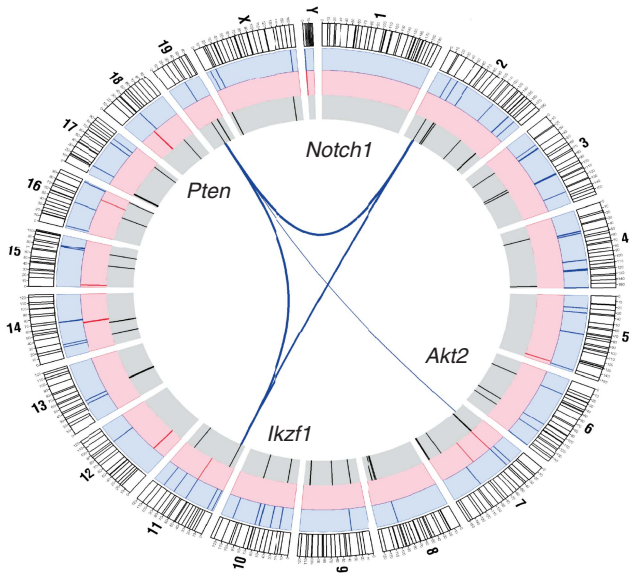

Figure 2. Analysis of common insertion sites. A Circos plot showing the common insertion sites (CISs) called in tumours from *Trp53*$^{+/+}$ (black), *Trp53*$^{+/-}$ (blue) and *Trp53*$^{-/-}$ (red) mice. Lines crossing the circle indicate statistically significant co-occurring mutations with the thickness of the line indicating the level of significance. All tumour DNA was extracted using GenePure kits (Qiagen, Sussex, UK) and transposon insertion site sequences were generated on the 454 platform (Roche, West Sussex, UK), as described previously.[30] Processing of 454 reads, identification of insertion sites, and the Gaussian Kernel Convolution statistical methods used to identify CISs have been described previously.[19,20] The *P*-value for each CIS was calculated using an adjusted-by-genome cutoff of $P<0.05$. A complete list of the CISs is given in Supplementary Table 1.

(*Mds1* and *Evi1* complex locus), *Myb*, *Notch1*, *Stat5b*, *Erg*, *Ikzf1*, *Raf1*, *Rasgrp1*, *Zmiz1*, *Pten*, *AB041803* and *Il2rb*. Given that eight of these genes have also been identified as CISs in leukaemias/lymphomas from *T2/Onc;Rosa26-SB11* mice on a wild-type background (*Myb*, *Notch1*, *Erg*, *Ikzf1*, *Rasgrp1*, *Zmiz1*, *Pten* and *AB041803*),[22] they likely represent genes involved in lymphomagenesis/leukemogenesis in general, and do not contribute to promotion of tumourigenesis in the context of *Trp53* heterozygosity.

A CIS gene that was found in the *Trp53*$^{+/-}$ and *Trp53*$^{-/-}$ tumours, but not *Trp53*$^{+/+}$ tumours, was *Rapgef6*. The Rap1 guanine nucleotide exchange factor RAPGEF6 (also known as PDZGEF2) has a critical role in the maturation of adherens junctions.[23] Although no immediate role for RAPGEF6 in tumourigenesis is evident, it has been shown to form protein complexes that result in the activation of Rap1A and control of cell adhesion/migration.[24,25] Interestingly, apart from *Rapgef6*, the CIS genes found in the *Trp53*$^{-/-}$ tumours were not found in tumours of the other genotypes. These included genes *Usp42* (ubiquitin specific peptidase 42) and *Wdr33* (WD repeat-containing protein 33). Although little is known about *Wdr33* gene, *Usp42* gene has been recently identified as a fusion partner of *RUNX1* in three cases of myeloid neoplasia, and the associated upregulated expression of USP42 suggests a role of this deubiquitinating enzyme in the pathogenesis of this leukaemia.[26]

There were also four CISs that were found to co-occur in tumours (Figure 2), specifically *Notch1* and *Pten*, *Notch1* and *Ikzf1*, *Pten* and *Ikzf1* and *Pten* and *Akt2* in *Trp53*$^{+/-}$ tumours. These genes have all been previously implicated in the pathogenesis of T-ALL.[21,27] Our results are in keeping with the literature, as there is evidence for genetic co-operation of these genes in development of T-ALL. For example, loss of *Ikzf1*, a direct repressor of Notch target genes, and suppression of p53-mediated apoptosis are essential for development of T-ALL and PTEN inactivation can compensate for some Notch-mediated processes in T-ALL.[21] In addition, retroviral insertional mutagenesis recently identified *Ikzf1*, *Kras*^{G12D} and *Notch1* as a novel genetic pathway in T-lineage leukaemogenesis.[28]

Quantitative PCR was performed on all tumours from *Trp53*$^{+/-}$ mice to identify those that had retained a wild-type copy of *Trp53* and those that carried two copies of the targeted *Trp53*^{Tyr} allele (presumably having lost the wild-type allele by mitotic recombination; Figure 3a). From the 111 *Trp53*$^{+/-}$ tumours analysed, we identified 40 that had retained a wild-type *Trp53* allele (defined as having a normalised wild-type allele content of >0.28 and a *Trp53*^{Tyr} allele content of <0.7) and 27 tumours that carried two targeted *Trp53*^{Tyr} alleles and no wild-type allele signal (defined as having a normalised wild-type allele content of <0.1 and a *Trp53*^{Tyr} allele content of >0.8). To determine if there were any somatic mutations in the intact wild-type copy of *Trp53*, genomic DNA from all 111 *Trp53*$^{+/-}$ tumours (as well as some tail samples to facilitate the identification of somatic mutations) underwent *Trp53* sequencing on the Illumina platform (Illumina, San Diego, CA, USA) to scan for point mutations (using the primers shown in Supplementary Table 2). Paired-end sequencing of PCR amplified fragments was followed by base-calling with SAMTOOLS mpileup,[29] which identified three possible mutations, specifically MMU11:69400422 (T-C), MMU11:69403089 (G-A) and MMU11:69403110 (G-A) in single tumours. All other tumours appeared to have retained the wild-type *Trp53* allele. A further two sequence changes at MMU11:69401065 and MMU11:69401996 were discovered in 22 and 44 of the samples, respectively, and are therefore likely to be germline variants (as these mice were on a mixed C57BL/6J-129Sv background and the sequencing data was compared with the C57BL/6J reference genome). These data suggest point mutations of the wild-type *Trp53* are infrequent in our model.

Taking the insertion sites found in tumours from *Trp53*$^{+/-}$ mice, we performed CIS analysis in two ways. First, the tumours were divided into two groups: those that had either retained a wild-type copy of *Trp53* or those that had lost the wild-type copy to identify the CISs that were unique and common to each group (Figure 3b). We found a set of nine CIS loci enriched in *Trp53*$^{+/-}$ mice that developed tumours despite retaining a wild-type copy of the gene, including *AB041803*, *Akt2*, *Eras*, *Ikzf1*, *Jdp2*, *Myb*, *Rapgef6* and two intergenic regions. Second, we pooled the insertion sites from both groups together and then distinguished genotype-specific CISs using a *P*-value generated by Fisher's Exact test analysis.[30] Using this more 'stringent' method of CIS calling, we identified two CISs that were 'enriched' in *Trp53*$^{+/-}$ tumours that had retained a wild-type copy of *Trp53*, specifically *AB041803* and *Jdp2*. Little is known about *AB041803* and as yet no role in tumourigenesis is evident. In addition, it was also found to be a CIS in leukaemia/lymphoma of wild-type mice (Supplementary Table 1).[22] Thus we focused on *Jdp2*.

Transcription factor JDP2 (also known as JUNDM2) is an AP-1 repressor protein[31] that has a paradoxical role in tumour formation. Overexpression of *Jdp2* has been shown to potentiate hepatocellular carcinoma in mice[32] and retroviral insertions predicted to activate the gene have been reported in mouse lymphoma models.[33,34] In contrast, downregulation of *JDP2* has been associated with a poor prognosis in pancreatic cancer.[35] Loss of *Jdp2* has also been associated with resistance to replicative senescence,[36,37] and *Jdp2* expression has been shown to suppress cell-cycle progression by downregulation of cyclin-A2.[38] However, hypomethylation of the *Jdp2* promoter or upregulation of *Jdp2* expression in common myeloid progenitors and in granulocyte-macrophage progenitors has led to suggestions that it functions as a regulator of myelopoiesis.[39] Here, we find that transposon insertions in the *Jdp2* promoter occur exclusively in tumours from *Trp53*$^{+/-}$ mice that retain a wild-type allele of *Trp53*. These

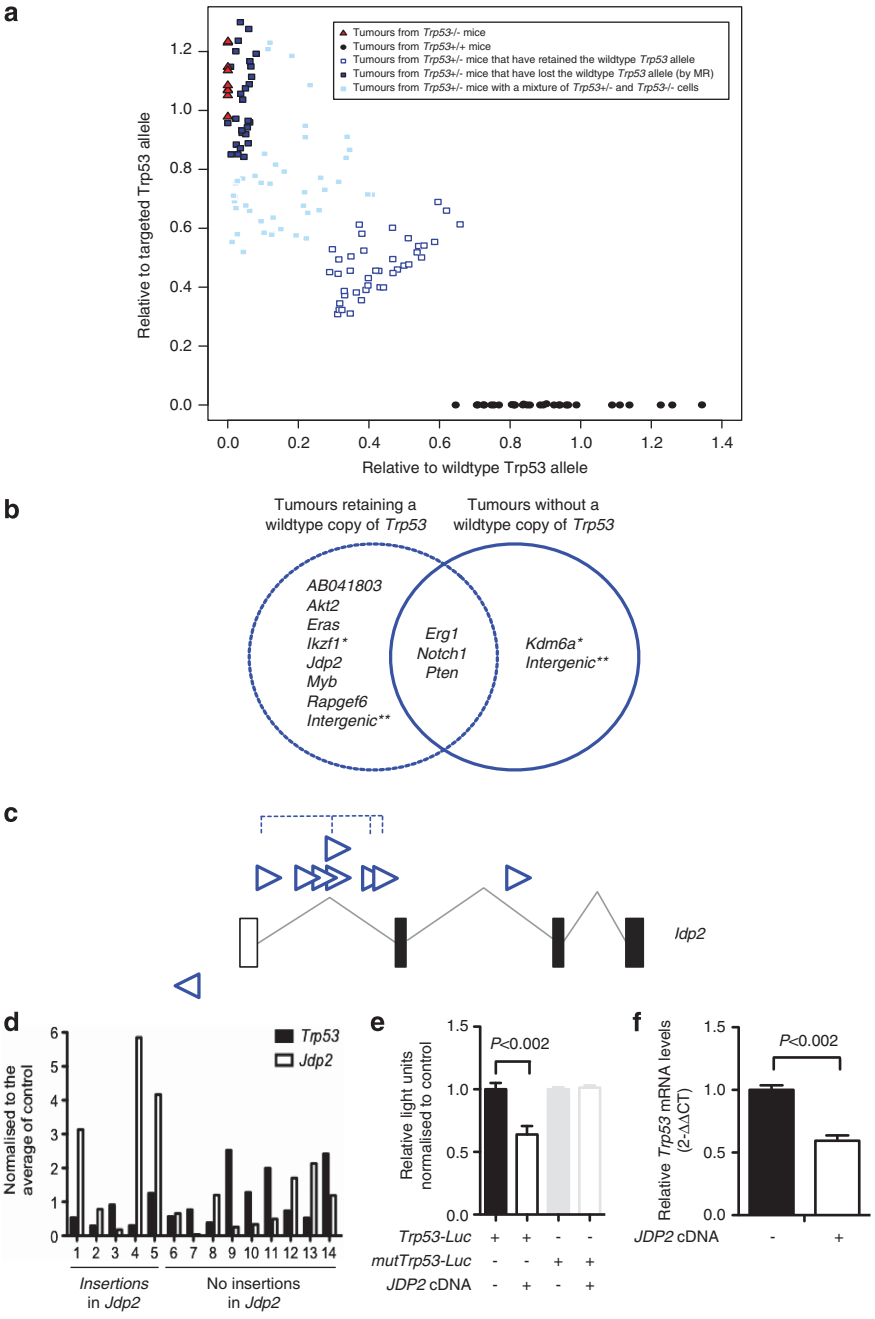

insertions clustered in the promoter of *Jdp2* (Figure 3c) and were mostly orientated so that the transposon was inserted in the same transcriptional orientation as the gene, suggesting that these insertions were functioning to drive overexpression (with a single insertion orientated on the reverse strand relative to the gene, which may represent an enhancer insertion[40]). RT–PCR on RNA from these tumours showed splicing of the T2Onc transposon splice donor site directly onto *Jdp2* exons 2 and/or 3 (Supplementary Figure 1). Indeed insertions in this exact location have been shown to activate *Jdp2* expression,[34] and consistent with this, qPCR on RNA from tumours containing insertions in *Jdp2* showed a trend towards having higher expression levels of *Jdp2* and lower expression levels of *Trp53*, relative to *Trp53*$^{+/-}$ tumours with no insertions in *Jdp2* (randomly selected from mice on this study that had not lost the *Trp53* allele by mitotic recombination; Figure 3d).

Co-transfection of *JDP2* cDNA in an overexpression vector with a mouse *Trp53* proximal promoter construct in murine NIH3T3 (Figure 3e) and human HEK293T cells (data not shown) resulted in significant repression of *Trp53* promoter activity, confirming that overexpression of *JDP2* functions directly on the *Trp53* promoter to repress *Trp53* expression. The ability of JDP2 to repress transcription of the *p53* promoter is reported to occur via its binding to an atypical AP-1 site, termed the PF-1 site, in the *p53* promoter.[41] When we mutated (deleted) this binding site in the proximal *Trp53* promoter, this completely abrogated the suppressive effects of *JDP2* (Figure 3e), confirming that overexpression of *JDP2* mediates repression of *Trp53* through the PF-1 site in the proximal promoter. Furthermore, overexpression of *JDP2* in HEK293T cells was shown to repress endogenous *TP53* expression (Figure 3f).

Figure 3. Identification of driver mutations associated with loss of *Trp53* by mitotic recombination or with the retention of a wild-type copy of *Trp53*. (**a**) SYBR Green quantitative real-time PCR (ABI, Carlsbad, CA, USA) was performed on tumour genomic DNA to quantify the relative proportions of *Trp53* wild-type and $Trp53^{Tyr}$ alleles in genomic DNA extracted from the leukaemias/lymphomas and data were normalised to the single-copy genes *β-Actin* and *Gapdh* (primers are detailed in Supplementary Table 3). Red triangles represent tumours from $Trp53^{-/-}$ mice, blue squares represent tumours from $Trp53^{+/-}$ mice and black circles represent tumours from $Trp53^{+/+}$ mice. Of the tumours from $Trp53^{+/-}$ mice: open squares are those that have retained a wild-type copy of *Trp53*, closed dark blue squares are those that have lost the wild-type *Trp53* allele by mitotic recombination (MR) and closed light blue squares are those with a mixture of $Trp53^{+/-}$ and $Trp53^{-/-}$ cells and thus were excluded from further analyses. (**b**). Common insertion sites (CISs) were identified in tumours from $Trp53^{+/-}$ mice that had retained a wild-type copy of *Trp53* (dotted blue circle) and those that had lost the wild-type copy (solid blue circle) as described previously.[19,20] CISs were called using a genome wide cut-off of $P<0.05$. Asterisk indicates the CIS was also found in the other genotype/circle, but below the $P<0.05$ cut-off. Double asterisk indicates the CISs were in intergenic regions (that is, not located within ± 150K base pairs of a gene and were given the label 'CIS' followed by the chromosome and the peak location of the Gaussian kernel; there were two regions for 'tumours retaining a wild-type copy of *Trp53*': CIS7:37317163_15k and CIS5:75854217_15k, and one for 'tumours without a wild-type copy of *Trp53*': CIS7:37322632_15k) (**c**). Location and orientation of the transposon insertions (blue triangles) associated with the *Jdp2* CIS (the exons of *Jdp2* are represented as boxes). One tumour was found to harbour multiple independent transposon insertion events (indicated with dotted lines). (**d**). Quantitative PCR (qPCR) was performed on five tumours containing insertions in *Jdp2* and nine randomly selected $Trp53^{+/-}$ T-cell tumours (without insertions in *Jdp2*). RNA was extracted using the RNeasy Minikit (Qiagen), DNAse-treated (Turbo DNase, Ambion, Warrington, UK) and reverse transcribed (RNA to cDNA EcoDry Random Hexamers, Clontech, Mountain View, CA, USA) according to the manufacturer's instructions. Quantitative PCR was performed in triplicate using SYBR Green PCR MasterMix (Applied Biosystems, Carlsbad, CA, USA) and the CT for *Trp53* and *Jdp2* were normalized to the 'control' (average of five housekeeping genes: *Gapdh*, *β-Actin*, *Hprt1*, *Rpl32* and *Rpl13a*) using the 2^{-CT} method.[42] Primers used for qPCR are given in Supplementary Table 4. (**e**). Transient overexpression of *JDP2* in NIH3T3 cells resulted in a significant repression of *Trp53* proximal promoter activity. The 375 bp mouse *Trp53* proximal promoter (*Trp53-Luc*) was PCR amplified from tail genomic DNA (using primers: F: 5′-AAAAAAAAGGTACCGGTCCACTTACGATAAAAAC-3′ and R: 5′-AAAAAAAAAA-GATCTGGTCCCAATGAACTGAAGCT-3′) and cloned into the pGL3-BASIC vector (Promega, Southhampton, UK). The mutated mouse *Trp53* proximal promoter in which the 7 bp PF-1 site (5′-TGACTCT-3′) was removed (*mutTrp53-Luc*) was synthesized (GeneArt-Invitrogen, Paisley, UK) and cloned into the pGL3-BASIC vector. A full-length human *JDP2* cDNA was obtained from Origene (Rockville, MD, USA). NIH3T3 cells grown in 96-well plates were transfected with (i) either 100 ng *Trp53-Luc* (black lines) or *mutTrp53-Luc* (grey lines), (ii) 20 ng pRL-SV40 (an internal control reporter; Promega) and (iii) either 50 ng *JDP2* cDNA or empty vector according to the manufacturer's instructions (Lipofectamine 2000; Invitrogen). Firefly and Renilla luciferase were measured 50 h later using the Dual-Luciferase Reporter Assay System according to the manufacturer's instructions (Promega). The firefly light units were normalised to the Renilla light units. All data were normalised to the average value of the 'control' transfection (*Luc* vector plus empty vector) and were presented as fold-change relative to the control. Experiments were performed in triplicate on at least three independent occasions and the data analysed by two-tailed Student's *t*-test. (**f**). Transient overexpression of *JDP2* in HEK293T cells represses *TRP53* expression. HEK293T cells (Gryphon Eco, Allele Biotechnology, San Diego, CA, USA) were seeded in 12-well plates and transfected with 2 μg Myc-DDK-tagged ORF clone of *JDP2* (pCMV6Entry; Origene) or empty vector, according to the manufacturers' instructions (Lipofectamine 2000, Invitrogen). Experiments were performed in triplicate. RNA was extracted 48 h post-transfection and reverse transcribed as described above. Quantitative PCR was performed in triplicate using SYBR Green PCR MasterMix (Applied Biosystems) and the CT for *TP53* and *JDP2* were normalized as described above. Primers used for qPCR are given in Supplementary Table 4.

In conclusion, we show that overexpression of *Jdp2* in tumours that are heterozygous for *Trp53* precludes the need for loss of the wild-type allele of *Trp53* during the process of leukaemogenesis. *Jdp2* overexpression is the first genetic mechanism that has been identified as being responsible for tumour formation in the context of *Trp53* heterozygosity.

CONFLICT OF INTEREST

The authors declare no conflict of interest.

ACKNOWLEDGEMENTS

DJA was supported by Cancer Research UK and the Wellcome Trust. LvdW was supported by the Kay Kendall Leukaemia Fund. CDRE was supported by Consejo Nacional de Ciencia y Tecnología (CONACYT) and the Wellcome Trust. MJA and REM were supported by Cancer Research UK.

REFERENCES

1 Levine AJ. p53, the cellular gatekeeper for growth and division. *Cell* 1997; **88**: 323 - 331.
2 Giaccia AJ, Kastan MB. The complexity of p53 modulation: emerging patterns from divergent signals. *Genes Dev* 1998; **12**: 2973 - 2983.
3 Olivier M, Hollstein M, Hainaut P. TP53 mutations in human cancers: origins, consequences, and clinical use. *Cold Spring Harb Perspect Biol* 2010; **2**: a001008.
4 Goh AM, Coffill CR, Lane DP. The role of mutant p53 in human cancer. *J Path* 2011; **223**: 116 - 126.
5 Robles AI, Harris CC. Clinical outcomes and correlates of TP53 mutations and cancer. *Cold Spring Harb Perspect Biol* 2010; **2**: a001016.
6 Trbusek M, Smardova J, Malcikova J, Sebejova L, Dobes P, Svitakova M *et al.* Missense mutations located in structural p53 DNA-binding motifs are associated with extremely poor survival in chronic lymphocytic leukemia. *J Clin Oncol* 2011; **29**: 2703 - 2708.
7 Venkatachalam S, Shi YP, Jones SN, Vogel H, Bradley A, Pinkel D *et al.* Retention of wild-type p53 in tumors from p53 heterozygous mice: reduction of p53 dosage can promote cancer formation. *EMBO J* 1998; **17**: 4657 - 4667.
8 Venkatachalam S, Tyner SD, Pickering CR, Boley S, Recio L, French JE *et al.* Is p53 haploinsufficient for tumor suppression? Implications for the p53+/- mouse model in carcinogenicity testing. *Toxicol Pathol* 2001; **29**: 147 - 154.
9 Donehower LA. Using mice to examine p53 functions in cancer, aging, and longevity. *Cold Spring Harb Perspect Biol* 2009; **1**: a001081.
10 Donehower LA, Lozano G. 20 years studying p53 functions in genetically engineered mice. *Nat Rev Cancer* 2009; **9**: 831 - 841.
11 Li FP, Fraumeni Jr JF. Soft-tissue sarcomas, breast cancer, and other neoplasms. A familial syndrome? *Ann Intern Med* 1969; **71**: 747 - 752.
12 Malkin D, Li FP, Strong LC, Fraumeni Jr JF, Nelson CE, Kim DH *et al.* Germ line p53 mutations in a familial syndrome of breast cancer, sarcomas, and other neoplasms. *Science* 1990; **250**: 1233 - 1238.
13 Sedlacek Z, Kodet R, Kriz V, Seemanova E, Vodvarka P, Wilgenbus P *et al.* Two Li-Fraumeni syndrome families with novel germline p53 mutations: loss of the wild-type p53 allele in only 50% of tumours. *Br J Cancer* 1998; **77**: 1034 - 1039.
14 Maiguel DA, Jones L, Chakravarty D, Yang C, Carrier F. Nucleophosmin sets a threshold for p53 response to UV radiation. *Mol Cell Biol* 2004; **24**: 3703 - 3711.
15 Zheng B, Vogel H, Donehower LA, Bradley A. Visual genotyping of a coat color tagged p53 mutant mouse line. *Cancer Biol Ther* 2002; **1**: 433 - 435.
16 Collier LS, Carlson CM, Ravimohan S, Dupuy AJ, Largaespada DA. Cancer gene discovery in solid tumours using transposon-based somatic mutagenesis in the mouse. *Nature* 2005; **436**: 272 - 276.
17 Dupuy AJ, Akagi K, Largaespada DA, Copeland NG, Jenkins NA. Mammalian mutagenesis using a highly mobile somatic Sleeping Beauty transposon system. *Nature* 2005; **436**: 221 - 226.
18 Uren AG, Mikkers H, Kool J, van der Weyden L, Lund AH, Wilson CH *et al.* A high-throughput splinkerette-PCR method for the isolation and sequencing of retroviral insertion sites. *Nat Protoc* 2009; **4**: 789 - 798.

19 de Ridder J, Uren A, Kool J, Reinders M, Wessels L. Detecting statistically significant common insertion sites in retroviral insertional mutagenesis screens. *PLoS Comput Biol* 2006; **2**: e166.
20 March HN, Rust AG, Wright NA, ten Hoeve J, de Ridder J, Eldridge M *et al.* Insertional mutagenesis reveals multiple networks of co-operating genes driving intestinal mutagenesis. *Nat Genet* 2011; **43**: 1202 - 1209.
21 Demarest RM, Ratti F, Capobianco AJ. It's T-ALL about Notch. *Oncogene* 2008; **27**: 5082 - 5091.
22 Collier LS, Adams DJ, Hackett CS, Bendzick LE, Akagi K, Davies MN *et al.* Whole-body sleeping beauty mutagenesis can cause penetrant leukemia/lymphoma and rare high-grade glioma without associated embryonic lethality. *Cancer Res* 2009; **69**: 8429 - 8437.
23 Dubé N, Kooistra MR, Pannekoek WJ, Vliem MJ, Oorschot V, Klumperman J *et al.* The RapGEF PDZ-GEF2 is required for maturation of cell-cell junctions. *Cell Signal* 2008; **20**: 1608 - 1615.
24 Severson EA, Lee WY, Capaldo CT, Nusrat A, Parkos CA. Junctional adhesion molecule A interacts with Afadin and PDZ-GEF2 to activate Rap1A, regulate beta1 integrin levels, and enhance cell migration. *Mol Biol Cell* 2009; **20**: 1916 - 1925.
25 Iwasaki M, Tanaka R, Hishiya A, Homma S, Reed JC, Takayama S. BAG3 directly associates with guanine nucleotide exchange factor of Rap1, PDZGEF2, and regulates cell adhesion. *Biochem Biophys Res Commun* 2010; **400**: 413 - 418.
26 Giguère A, Hébert J. Microhomologies and topoisomerase II consensus sequences identified near the breakpoint junctions of the recurrent t(7;21)(p22;q22) translocation in acute myeloid leukemia. *Genes Chromosomes Cancer* 2011; **50**: 228 - 238.
27 Gutierrez A, Grebliunaite R, Feng H, Kozakewich E, Zhu S, Guo F *et al.* Pten mediates Myc oncogene dependence in a conditional zebrafish model of T cell acute lymphoblastic leukemia. *J Exp Med* 2011; **208**: 1595 - 1603.
28 Dail M, Li Q, McDaniel A, Wong J, Akagi K, Huang B *et al.* Mutant Ikzf1, KrasG12D, and Notch1 cooperate in T lineage leukemogenesis and modulate responses to targeted agents. *Proc Natl Acad Sci USA* 2010; **107**: 5106 - 5111.
29 Li H, Handsaker B, Wysoker A, Fennell T, Ruan J, Homer N *et al.* The Sequence Alignment/Map format and SAMtools. *Bioinformatics* 2009; **25**: 2078 - 2079.
30 Uren AG, Kool J, Matentzoglu K, de Ridder J, Mattison J, van Uitert M *et al.* Large-scale mutagenesis in p19(ARF)- and p53-deficient mice identifies cancer genes and their collaborative networks. *Cell* 2008; **133**: 727 - 741.
31 Aronheim A, Zandi E, Hennemann H, Elledge SJ, Karin M. Isolation of an AP-1 repressor by a novel method for detecting protein-protein interactions. *Mol Cell Biol* 1997; **17**: 3094 - 3102.
32 Bitton-Worms K, Pikarsky E, Aronheim A. The AP-1 repressor protein, JDP2, potentiates hepatocellular carcinoma in mice. *Mol Cancer* 2010; **9**: 54.
33 Stewart M, Mackay N, Hanlon L, Blyth K, Scobie L, Cameron E *et al.* Insertional mutagenesis reveals progression genes and checkpoints in MYC/Runx2 lymphomas. *Cancer Res* 2007; **67**: 5126 - 5133.
34 Rasmussen MH, Wang B, Wabl M, Nielsen AL, Pedersen FS. Activation of alternative Jdp2 promoters and functional protein isoforms in T-cell lymphomas by retroviral insertion mutagenesis. *Nuc Acids Res* 2009; **37**: 4657 - 4671.
35 Yuanhong X, Feng X, Qingchang L, Jianpeng F, Zhe L, Kejian G. Downregulation of AP-1 repressor JDP2 is associated with tumor metastasis and poor prognosis in patients with pancreatic carcinoma. *Int J Biol Markers* 2010; **25**: 136 - 140.
36 Nakade K, Pan J, Yamasaki T, Murata T, Wasylyk B, Yokoyama KK. JDP2 (Jun Dimerization Protein 2)-deficient mouse embryonic fibroblasts are resistant to replicative senescence. *J Biol Chem* 2009; **284**: 10808 - 10817.
37 Wang SW, Lee JK, Ku CC, Chiou SS, Ho MF, Wu DC *et al.* Jun dimerization protein 2 in oxygen restriction; control of senescence. *Curr Pharm Des* 2011; **17**: 2278 - 2289.
38 Pan J, Nakade K, Huang YC, Zhu ZW, Masuzaki S, Hasegawa H *et al.* Suppression of cell-cycle progression by Jun dimerization protein-2 (JDP2) involves down-regulation of cyclin-A2. *Oncogene* 2010; **29**: 6245 - 6256.
39 Ji H, Ehrlich LI, Seita J, Murakami P, Doi A, Lindau P *et al.* Comprehensive methylome map of lineage commitment from haematopoietic progenitors. *Nature* 2010; **467**: 338 - 342.
40 Uren AG, Kool J, Berns A, van Lohuizen M. Retroviral insertional mutagenesis: past, present and future. *Oncogene* 2005; **24**: 7656 - 7672.
41 Piu F, Aronheim A, Katz S, Karin M. AP-1 repressor protein JDP-2: inhibition of UV-mediated apoptosis through p53 down-regulation. *Mol Cell Biol* 2001; **21**: 3012 - 3024.
42 Livak KJ, Schmittgen TD. Analysis of relative gene expression data using real-time quantitative PCR and the 2(-Delta Delta C(T)) Method. *Methods* 2001; **25**: 402 - 408.

Supplementary Information accompanies the paper on the Oncogene website (http://www.nature.com/onc)